

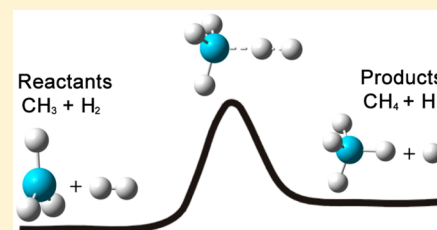
Time-Dependent Wave Packet Study of the $\text{H}_2 + \text{CH}_3 \rightarrow \text{H} + \text{CH}_4$ Reaction

Zhaojun Zhang,[†] Jun Chen,[†] Minghui Yang,^{*,‡} and Dong H. Zhang^{*,†}

[†]State Key Laboratory of Molecular Reaction Dynamics and Center for Theoretical Computational Chemistry, Dalian Institute of Chemical Physics, Chinese Academy of Sciences, Dalian 116023, People's Republic of China

[‡]State Key Laboratory of Magnetic Resonance and Atomic and Molecular Physics, National Centre for Magnetic Resonance in Wuhan, Wuhan Institute of Physics and Mathematics, Chinese Academy of Sciences, Wuhan 430071, China

ABSTRACT: The initial state selected time-dependent wave packet method has been developed to study the $\text{H}_2 + \text{CH}_3 \rightarrow \text{H} + \text{CH}_4$ reaction, by employing the seven- and eight-dimensional models proposed by Palma and Clary in which the nonreacting CH_3 moiety is restricted in C_{3v} symmetry. Total reaction probabilities and integral cross sections were calculated for the ground and a number of vibrationally excited initial states to investigate the effects of vibrational excitations of both reagents on the reaction. The eight-dimensional calculations showed that the CH stretching excitation does not have any important effect on the reaction and the seven-dimensional model with the CH bond length fixed works very well for the reaction. The excitation of H_2 vibrations could enhance the reaction but is less effective than the translation in the low energy region. In contrast, the first umbrella excitation is very effective on reducing the reaction threshold. The calculated rate constants are found to be in good agreement with available experimental measurements and other theoretical results.



In the past two decades, significant progress has been made on accurate quantum reactive scattering studies of gas-phase chemical reactions, largely through the development of the time-dependent wave packet method (TDWP). Now it is possible to calculate state-to-state differential cross sections (DCS) for most triatomic reactions. Recently, the TDWP method has been developed to compute state-to-state DCS for some simple tetra-atomic reactions without any dynamical approximation, with excellent agreements achieved between theory and high-resolution crossed-molecular beam experiments.^{1–3}

One of the major challenges in the field of quantum reaction dynamics is to develop accurate yet affordable methods to study polyatomic chemical reactions involving more than four atoms, such as the $\text{H} + \text{CH}_4 \rightarrow \text{H}_2 + \text{CH}_3$ reaction. Due to its important role in CH_4/O_2 combustion chemistry, the reaction has been widely studied experimentally and theoretically. Because there are five hydrogen atoms involved, the reaction system has become a benchmark system to test various dynamical methods for polyatomic reactions. Yu and Nyman employed rotating bond approximation (RBA) method to include the floppy umbrella modes of CH_3 .⁴ Wang and Bowman studied this reaction with a six-dimensional (6D) time-dependent wave packet study by approximating the three hydrogen atoms in CH_3 as a pseudoatom.⁵ Zhang and co-workers developed a semirigid vibrating rotor target (SVRT) model to study reaction.⁶ Using the multiconfiguration time-dependent Hartree (MCTDH) method, Manthe and co-workers have performed a series of full-dimensional quantum dynamics studies on reaction.^{7–18} Starting from calculating the cumulative reaction probabilities for the total angular momentum $J = 0$ from which the thermal rate constants can

be estimated reliably, they managed to obtain initial state-selected and even state-to-state reaction probabilities for the title reaction in low collision energy region by propagate the wave packets back and forth from the transition state region.^{16–18}

In 2000, Palma and Clary proposed an eight-dimensional model to deal with reactions of the type $\text{X} + \text{YCZ}_3 \rightarrow \text{XY} + \text{CZ}_3$.¹⁹ It is a full-dimensional model for the type of reactions under the assumption that the CZ_3 group keeps a C_{3v} symmetry in the reaction. Because the assumption is expected to hold very well in reality, it is the most realistic reduced-dimensionality model developed so far in calculating the initial state selected reaction probability. Yang and Zhang implemented the model by using the time-dependent wave packet method in 2002. Since then, the model has been applied extensively to study many reactions such as $\text{H} + \text{CH}_4$,^{20–23} $\text{O} + \text{CH}_4$,^{24,25} $\text{H} + \text{CD}_4$,²⁶ $\text{H} + \text{CHD}_3$,^{27–29} and $\text{Cl} + \text{CHD}_3$,^{30,31} and provided some results in good agreement with experimental.^{26,30}

In contrast, the $\text{H}_2 + \text{CH}_3 \rightarrow \text{H} + \text{CH}_4$ reaction has not been so extensively studied as its reverse counterpart. Besides the full-dimensional MCTDH calculation of thermal rate constants of the reaction by Manthe and co-workers,³² there were only a few studies based on classical mechanics and reduced dimensional quantum dynamics. Wang has presented a six-dimensional quantum dynamics method to study the title

Special Issue: Dynamics of Molecular Collisions XXV: Fifty Years of Chemical Reaction Dynamics

Received: August 14, 2015

Revised: October 23, 2015

reaction by treating the CH_3 as a diatomic molecule.³³ In this work, Wang employed the same approximation as in their study of the $\text{H} + \text{CH}_4 \rightarrow \text{H}_2 + \text{CH}_3$ reaction by treating the CH_3 moiety as a pseudodiatom molecule.⁵ Recently, Wang and co-workers extended the model to seven dimensions to study the $\text{OH} + \text{CH}_3 \rightarrow \text{O} + \text{CH}_4$ reaction by treating the CH_3 moiety as a collinear triatomic molecule HCX .³⁴

In this letter, we report seven- and eight-dimensional quantum dynamics studies for the $\text{H}_2 + \text{CH}_3 \rightarrow \text{H} + \text{CH}_4$ reaction. The eight-dimensional model of Palma and Clary was employed, with the symmetric stretch and umbrella motions of CH_3 being treated explicitly. The 8D Hamiltonian proposed by Yang et al. recently was employed here to treat the CH_3 group.²¹ This vibrational Hamiltonian of CH_3 group, expressed in a set of scaled polar coordinates, is considerably simpler than the previous form.²³ We used a total of 120 sine functions (including 48 for the interaction region) for the translational coordinate R in a range of $[2.0, 15.0] a_0$, and 6 and 40 basis functions were used for H_2 stretch in the asymptotic and interaction regions, respectively. Fifteen basis functions were used for the umbrella motion of CH_3 and three basis functions for CH stretching. In the 7D calculations, the length of CH bond was fixed at its equilibrium value of $2.036 a_0$. The same set of rotational basis functions were used for both 7D and 8D calculations: $j_{\text{max}} = 30$ and $k_{\text{max}} = 3$ were used for CH_3 rotation where j_{max} and k_{max} have the same meaning as that in the studies of $\text{H} + \text{CH}_4 \rightarrow \text{H}_2 + \text{CH}_3$ reaction, $l_{\text{max}} = 30$ was used for H_2 rotation. The total number of rotational basis functions is 30 016 for even parity considered in this study. The potential energy surface (PES) employed in the present study was constructed very recently in this group by using neural network fitting to about 48 000 *ab initio* energies calculated at UCCSD(T)-F12/AVTZ level.³⁵

Figure 1 shows the $J_{\text{tot}} = 0$ total reaction probabilities as a function of translational energy with reagent H_2 and CH_3 in different initial vibrational states. In the 7D calculations, an initial vibrational state is labeled as (v_{H_2}, v_u) , where v_{H_2} and v_u represents the vibrational state of H_2 and the umbrella state of

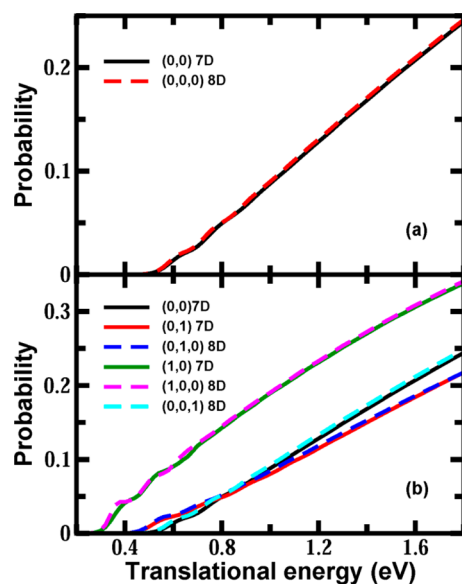


Figure 1. Total reaction probabilities ($J_{\text{tot}} = 0$) as a function of translational energy with reagents initially in different vibrational states (v_{H_2}, v_u) and $(v_{\text{H}_2}, v_u, v_s)$ for 7D and 8D, respectively.

CH_3 , respectively. On the PES used in this study, the excitation energy of first excited state of H_2 is 4158.7 cm^{-1} with the zero point energy (ZPE) of 2178.15 cm^{-1} , and the excitation energy of the first excited state of CH_3 umbrella motion is 640.5 cm^{-1} with the ZPE of 294.8 cm^{-1} . In the 8D calculations, an initial vibrational states is labeled as $(v_{\text{H}_2}, v_u, v_s)$, with v_s representing the symmetric stretch motion of CH_3 . In the 8D model, the ZPE of CH_3 is 1841.2 cm^{-1} and the excitation energy of the first excited state $(0, 1, 0)$ of CH_3 umbrella motion is 623.7 cm^{-1} and the excitation energy of the first excited state $(0, 0, 1)$ of CH_3 stretch motion is 3070.3 cm^{-1} . As can be seen from Figure 1a, the 8D reaction probability for the ground initial state has a threshold energy of $\sim 0.51 \text{ eV}$ and increases essentially linearly with the collision energy. It reaches 0.24 at the collision energy of 1.8 eV , much larger than the reaction probability for the reverse $\text{H} + \text{CH}_4$ reaction. The 7D reaction probability is almost identical to the 8D result, except a tiny shift of threshold energy of about 0.01 eV to high energy. As seen from Figure 1b, the 8D probabilities for $(0, 1, 0)$ and $(1, 0, 0)$ initial vibrational states are almost the same as the corresponding 7D ones. Furthermore, we also can see the probability for the first symmetric stretch excitation of CH_3 $(0, 0, 1)$ state is very close to the probability of the 7D ground initial state. These results clearly show the CH stretch motion in the nonreactive CH_3 group is a spectator mode in the reaction and can be frozen in dynamical calculations without introducing any noticeable error. As a result, we will use the 7D model to compute the ICS for the reaction. Also can be seen from Figure 1b the H_2 vibrational excitation enhances the reactivity considerably, whereas the umbrella excitation of CH_3 group only enhances the reactivity in low collision energy region. Finally, it is interesting to note that all the probabilities in Figure 1 have some oscillation structures at the low energy region, in particular for the 8D $(1, 0, 0)$ initial state.

Figure 2a presents the 7D ICSs for some initial states as a function of translational energy. The maximum value of J_{tot}

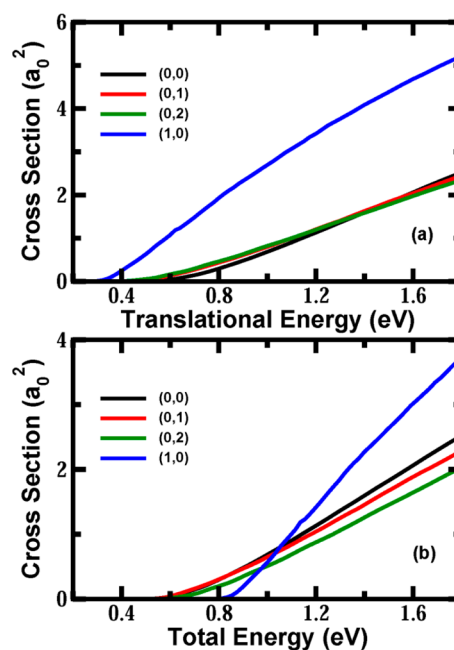


Figure 2. (a) Integral cross sections for 7D different initial states (v_{H_2}, v_u) as a function of translational energy. (b) Same as (a), but as a function of total energy.

needed to converge the integral cross section in the energy region considered here is 75, and the centrifugal sudden (CS) approximation is employed for the $J_{\text{tot}} > 0$ reaction probability calculation. It can be seen that the behaviors of the cross sections are very similar to those of the reaction probabilities shown in Figure 1. At the same collision energy, the initial vibrational excitation of H_2 enhances the cross sections substantially, in particular in the low collision energy region. At the collision energy of 1.8 eV, the ICS of (1, 0) initial state is about double that for the ground state. The umbrella excitations have less effect on the cross sections, in particular in the high collision energy region. The first umbrella excitation reduces the threshold energy noticeably; in contrast, the second umbrella excitation only reduces the threshold by a small amount. For the higher umbrella excitation states, the ICSs are similar to the ICS of the (0, 2) state shown in the figure. Welsh and Manthe recently found in their MCTDH based full-dimensional state-to-state quantum dynamics study on the $\text{H} + \text{CH}_4 \rightarrow \text{H}_2 + \text{CH}_3$ that there is a substantial amount of CH_3 produced in the umbrella excited states, in particular in the first excited one,¹⁸ in line with the results found here.

When measured as a function of total energy as shown in Figure 2b, the ICS for the (1, 0) initial state has a crossover point with the ICS of the ground state at the total energy of about 1.05 eV. This means that at the low total energy the translational energy is more effective on promoting the reaction than the H_2 vibrational excitation, whereas at the high total energy the H_2 vibrational excitation is more effective. On the PES used in this study, the transition state for the title reaction has a collinear geometry with the H_2 bond stretched to $1.69 a_0$ and the new forming CH bond length of $2.64 a_0$, in comparison with the equilibrium value of $1.41 a_0$ for H_2 and $2.05 a_0$ for CH in CH_4 . Therefore, the title reaction has a slightly early barrier, and the lower efficiency of the H_2 vibrational excitation on prompting the reaction over the translational energy in the low energy region observed here is in accordance with the Polanyi rules. This is also in good agreement with the prediction given by the sudden vector projection (SVP) model proposed by Guo and co-workers,^{36,37} which gives 0.62 for H_2 vibrational motion and 0.71 for the translational motion.

For the umbrella excitation, the ICS for the (0, 2) state is smaller than that for the ground initial state in the entire energy region, whereas the ICS for the (0, 1) state is very close to that for the ground state for total energy less than 0.9 eV and becomes slightly less than that at higher energy region. This means that at low collision energy the energy deposited in the first CH_3 umbrella excited state has the same efficacy as the translational energy, in contradiction with the SVP model which predicts 0.33 for umbrella motion. At the transition state, the CH_3 group has an umbrella angle (the angle between a CH bond and the C_3 axis) of 77° , in comparison with 90° for CH_3 radical. Therefore, the umbrella angle changes considerably from reagent to saddle point, and it is not surprising to see the umbrella excitation can reduce the reaction threshold effectively.

In Figure 3 we show the vibrational state averaged rate constants for the title reaction together with the transition state theory (TST), full-dimensional MCTDH,³² and eight-dimensional transition state wave packet (TSWP) results,³⁸ in comparison with experimental measurements.^{39–42} Because the excitation energies for the umbrella motion of CH_3 are quite different from the corresponding harmonic energies, we used 15 umbrella excited energies of CH_3 yielded from the 7D

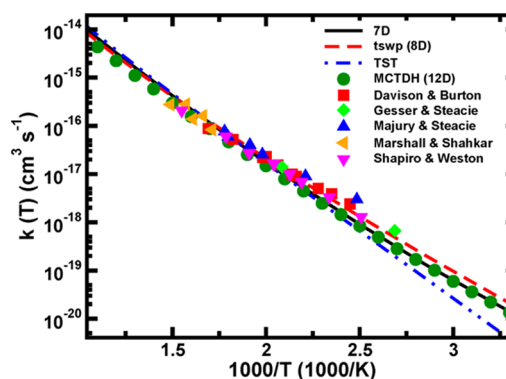


Figure 3. Comparison between the present rate constant for 7D initial state-selected with other theoretical and available experimental results.

model to obtain the CH_3 vibrational partition function for the TST rate constant calculation. The partition function for the umbrella mode under the harmonic approximation is about 17% larger than that calculated in this way at the temperature of 1000 K. Because the 7D and 8D probabilities agree with each other extremely well, as shown in Figure 1, we only calculate the rate constants on the basis of the 7D model. As expected, TST noticeably underestimated the rates at low temperatures, but the overall agreements between various theoretical results, and between theory and experiment, are satisfactory. It is worthwhile to point out that the PES used in the MCTDH calculation was different from that used in this study. The good agreement between these two studies indicates both PESs are very close on the level of accuracy for describing the reaction. Finally, one may note that the present 7D rate constant is very close to the TSWP rate constant in the high temperature region, but their ratio reaches about 1.5 at $T = 300$ K. This discrepancy may be attributed to the following two reasons: one is the CS approximations employed in the present study, the other is the effects of reagents rotation excitation, which was not included in this work but was included in the TSWP study. Further studies should be carried out to examine the accuracy of the CS approximation to the reaction and to investigate the effects of reagent rotation excitation of the reaction.

In summary, an eight-dimensional time-dependent wave packet method was developed to study the $\text{H}_2 + \text{CH}_3 \rightarrow \text{H} + \text{CH}_4$ reaction, based on Palma and Clary's model in which the nonreacting CH_3 moiety keeps C_{3v} symmetry. Our calculations showed that the CH stretch mode is a spectator in the reaction; therefore, the CH bond length can be fixed in calculation without introducing any noticeable error. The H_2 vibration excitation could enhance the reaction considerably but is still less effective than the translational energy in the low energy region, in accord with the Polanyi rules for an early barrier reaction and the SVP model. The effect of the umbrella excitation of CH_3 on the reaction is more complicated. Only for the first excited state can the entire energy deposited in the umbrella motion be used to reduce the threshold energy, making the umbrella excitation have the same efficacy on prompting the reaction as the translational energy. The efficacy decreases with the increase of excitation level of the umbrella motion. Overall, the calculated rate constants agree well with the experimental and other theoretical values. This work presents a useful tool for the $\text{XY} + \text{CZ}_3 \rightarrow \text{X} + \text{YCZ}_3$ type reaction.

■ AUTHOR INFORMATION

Corresponding Authors

*M. Yang. E-mail: yangmh@wipm.ac.cn.

*D. H. Zhang. E-mail: zhangdh@dicp.ac.cn.

Notes

The authors declare no competing financial interest.

■ ACKNOWLEDGMENTS

D.H.Z. acknowledges the support by the National Science Foundation of China (Grant No. 91221301 and 91421315), Ministry of Science and Technology of China (2013CB834601), and Chinese Academy of Sciences, and M.Y. acknowledges the supported by the National Science Foundation of China (Grant No. 21373266 and 21221064).

■ REFERENCES

- (1) Xiao, C.; Xu, X.; Liu, S.; Wang, T.; Dong, W.; Yang, T.; Sun, Z.; Dai, D.; Xu, X.; Zhang, D. H.; Yang, X. Experimental and theoretical differential cross sections for a four-atom reaction: $\text{HD} + \text{OH} \rightarrow \text{H}_2\text{O} + \text{D}$. *Science* **2011**, *333*, 440–442.
- (2) Liu, S.; Xu, X.; Zhang, D. H. Time-dependent wave packet theory for state-to-state differential cross sections of four-atom reactions in full dimensions: Application to the $\text{HD} + \text{OH} \rightarrow \text{H}_2\text{O} + \text{D}$ reaction. *J. Chem. Phys.* **2012**, *136*, 144302.
- (3) Liu, S.; Xiao, C. L.; Wang, T.; Chen, J.; Yang, T. G.; Xu, X.; Zhang, D. H.; Yang, X. M. The dynamics of the $\text{D}_2 + \text{OH} \rightarrow \text{HOD} + \text{D}$ reaction: A combined theoretical and experimental study. *Faraday Discuss.* **2012**, *157*, 101–111.
- (4) Yu, H. G.; Nyman, G. Four-dimensional quantum scattering calculations on the $\text{H} + \text{CH}_4 \rightarrow \text{H}_2 + \text{CH}_3$ reaction. *J. Chem. Phys.* **1999**, *111*, 3508–3516.
- (5) Wang, D. Y.; Bowman, J. M. A reduced dimensionality, six-degree-of-freedom, quantum calculation of the $\text{H} + \text{CH}_4 \rightarrow \text{H}_2 + \text{CH}_3$ reaction. *J. Chem. Phys.* **2001**, *115*, 2055–2061.
- (6) Wang, M. L.; Zhang, J. Z. H. Generalized semirigid vibrating rotor target model for atom-poly reaction: Inclusion of umbrella mode for $\text{H} + \text{CH}_4$ reaction. *J. Chem. Phys.* **2002**, *117*, 3081–3087.
- (7) Wu, T.; Werner, H. J.; Manthe, U. First-principles theory for the $\text{H} + \text{CH}_4 \rightarrow \text{H}_2 + \text{CH}_3$ reaction. *Science* **2004**, *306*, 2227–2229.
- (8) Wu, T.; Werner, H. J.; Manthe, U. Accurate potential energy surface and quantum reaction rate calculations for the $\text{H} + \text{CH}_4 \rightarrow \text{H}_2 + \text{CH}_3$ reaction. *J. Chem. Phys.* **2006**, *124*, 164307.
- (9) van Harrevelt, R.; Nyman, G.; Manthe, U. Accurate quantum calculations of the reaction rates for $\text{H}/\text{D} + \text{CH}_4$. *J. Chem. Phys.* **2007**, *126*, 084303.
- (10) Schiffel, G.; Manthe, U. A transition state view on reactive scattering: Initial state-selected reaction probabilities for the $\text{H} + \text{CH}_4 \rightarrow \text{H}_2 + \text{CH}_3$ reaction studied in full dimensionality. *J. Chem. Phys.* **2010**, *133*, 174124.
- (11) Schiffel, G.; Manthe, U. Communications: A rigorous transition state based approach to state-specific reaction dynamics: Full-dimensional calculations for $\text{H} + \text{CH}_4 \rightarrow \text{H}_2 + \text{CH}_3$. *J. Chem. Phys.* **2010**, *132*, 191101.
- (12) Schiffel, G.; Manthe, U. Quantum dynamics of the $\text{H} + \text{CH}_4 \rightarrow \text{H}_2 + \text{CH}_3$ reaction in curvilinear coordinates: Full-dimensional and reduced dimensional calculations of reaction rates. *J. Chem. Phys.* **2010**, *132*, 084103.
- (13) Schiffel, G.; Manthe, U.; Nyman, G. Full-dimensional quantum reaction rate calculations for $\text{H} + \text{CH}_4 \rightarrow \text{H}_2 + \text{CH}_3$ on a recent potential energy surface. *J. Phys. Chem. A* **2010**, *114*, 9617–9622.
- (14) Welsch, R.; Manthe, U. Reaction dynamics with the multi-layer multi-configurational time-dependent Hartree approach: $\text{H} + \text{CH}_4 \rightarrow \text{H}_2 + \text{CH}_3$ rate constants for different potentials. *J. Chem. Phys.* **2012**, *137*, 244106.
- (15) Welsch, R.; Manthe, U. Communication: Ro-vibrational control of chemical reactivity in $\text{H} + \text{CH}_4 \rightarrow \text{H}_2 + \text{CH}_3$: Full-dimensional quantum dynamics calculations and a sudden model. *J. Chem. Phys.* **2014**, *141*, 051102.
- (16) Welsch, R.; Manthe, U. The role of the transition state in polyatomic reactions: Initial state-selected reaction probabilities of the $\text{H} + \text{CH}_4 \rightarrow \text{H}_2 + \text{CH}_3$ reaction. *J. Chem. Phys.* **2014**, *141*, 174313.
- (17) Welsch, R.; Manthe, U. Full-dimensional and reduced-dimensional calculations of initial state-selected reaction probabilities studying the $\text{H} + \text{CH}_4 \rightarrow \text{H}_2 + \text{CH}_3$ reaction on a neural network PES. *J. Chem. Phys.* **2015**, *142*, 064309.
- (18) Welsch, R.; Manthe, U. Loss of memory in $\text{H} + \text{CH}_4 \rightarrow \text{H}_2 + \text{CH}_3$ state-to-state reactive scattering. *J. Phys. Chem. Lett.* **2015**, *6*, 338–342.
- (19) Palma, J.; Clary, D. C. A quantum model Hamiltonian to treat reactions of the type $\text{X} + \text{YCZ}_3 \rightarrow \text{XY} + \text{CZ}_3$: Application to $\text{O}(^3\text{P}) + \text{CH}_4 \rightarrow \text{OH} + \text{CH}_3$. *J. Chem. Phys.* **2000**, *112*, 1859–1867.
- (20) Yang, M. H.; Zhang, D. H.; Lee, S. Y. A seven-dimensional quantum study of the $\text{H} + \text{CH}_4$ reaction. *J. Chem. Phys.* **2002**, *117*, 9539–9542.
- (21) Liu, R.; Xiong, H. W.; Yang, M. H. An eight-dimensional quantum mechanical Hamiltonian for $\text{X} + \text{YCZ}_3$ system and its applications to $\text{H} + \text{CH}_4$ reaction. *J. Chem. Phys.* **2012**, *137*, 174113.
- (22) Liu, S.; Chen, J.; Zhang, Z. J.; Zhang, D. H. Communication: A six-dimensional state-to-state quantum dynamics study of the $\text{H} + \text{CH}_4 \rightarrow \text{H}_2 + \text{CH}_3$ reaction ($J = 0$). *J. Chem. Phys.* **2013**, *138*, 011101.
- (23) Zhang, L.; Lu, Y.; Lee, S.-Y.; Zhang, D. H. A transition state wave packet study of the $\text{H} + \text{CH}_4$ reaction. *J. Chem. Phys.* **2007**, *127*, 234313.
- (24) Yang, M. H.; Lee, S. Y.; Zhang, D. H. Seven-dimensional quantum dynamics study of the $\text{O}(^3\text{P}) + \text{CH}_4$ reaction. *J. Chem. Phys.* **2007**, *126*, 064303.
- (25) Liu, R.; Yang, M. H.; Czako, G.; Bowman, J. M.; Li, J.; Guo, H. Mode selectivity for a “Central” barrier reaction: eight-dimensional quantum studies of the $\text{O}(^3\text{P}) + \text{CH}_4 \rightarrow \text{OH} + \text{CH}_3$ reaction on an ab initio potential energy surface. *J. Phys. Chem. Lett.* **2012**, *3*, 3776–3780.
- (26) Zhang, W. Q.; Zhou, Y.; Wu, G. R.; Lu, Y. P.; Pan, H. L.; Fu, B. N.; Shuai, Q. A.; Liu, L.; Liu, S.; Zhang, L. L.; Jiang, B.; Dai, D. X.; Lee, S. Y.; Xie, Z.; Braams, B. J.; Bowman, J. M.; Collins, M. A.; Zhang, D. H.; Yang, X. M. Depression of reactivity by the collision energy in the single barrier $\text{H} + \text{CD}_4 \rightarrow \text{HD} + \text{CD}_3$ reaction. *Proc. Natl. Acad. Sci. U. S. A.* **2010**, *107*, 12782–12785.
- (27) Zhou, Y.; Wang, C. R.; Zhang, D. H. Effects of reagent vibrational excitation on the dynamics of the $\text{H} + \text{CHD}_3 \rightarrow \text{H}_2 + \text{CD}_3$ reaction: A seven-dimensional time-dependent wave packet study. *J. Chem. Phys.* **2011**, *135*, 024313.
- (28) Zhang, Z. J.; Chen, J.; Liu, S.; Zhang, D. H. Accuracy of the centrifugal sudden approximation in the $\text{H} + \text{CHD}_3 \rightarrow \text{H}_2 + \text{CD}_3$ reaction. *J. Chem. Phys.* **2014**, *140*, 224304.
- (29) Zhang, Z.; Zhang, D. H. Effects of reagent rotational excitation on the $\text{H} + \text{CHD}_3 \rightarrow \text{H}_2 + \text{CD}_3$ reaction: A seven dimensional time-dependent wave packet study. *J. Chem. Phys.* **2014**, *141*, 144309.
- (30) Zhang, Z. J.; Zhou, Y.; Zhang, D. H.; Czako, G.; Bowman, J. M. Theoretical study of the validity of the polanyi rules for the late-barrier $\text{Cl} + \text{CHD}_3$ reaction. *J. Phys. Chem. Lett.* **2012**, *3*, 3416–3419.
- (31) Liu, R.; Wang, F. Y.; Jiang, B.; Czako, G.; Yang, M. H.; Liu, K. P.; Guo, H. Rotational mode specificity in the $\text{Cl} + \text{CHD}_3 \rightarrow \text{HCl} + \text{CD}_3$ reaction. *J. Chem. Phys.* **2014**, *141*, 074310.
- (32) Nyman, G.; van Harrevelt, R.; Manthe, U. Thermochemistry and accurate quantum reaction rate calculations for $\text{H}_2/\text{HD}/\text{D}_2 + \text{CH}_3$. *J. Phys. Chem. A* **2007**, *111*, 10331–10337.
- (33) Wang, D. Y. A time-dependent quantum dynamics study of the $\text{H}_2 + \text{CH}_3 \rightarrow \text{H} + \text{CH}_4$ reaction. *J. Chem. Phys.* **2002**, *117*, 9806–9810.
- (34) Yan, P.; Wang, Y.; Li, Y.; Wang, D. A seven-degree-of-freedom, time-dependent quantum dynamics study on the energy efficiency in surmounting the central energy barrier of the $\text{OH} + \text{CH}_3 \rightarrow \text{O} + \text{CH}_4$ reaction. *J. Chem. Phys.* **2015**, *142*, 164303.
- (35) Xu, X.; Chen, J.; Zhang, D. H. Global potential energy surface for the $\text{H} + \text{CH}_4 \leftrightarrow \text{H}_2 + \text{CH}_3$ reaction using neural networks. *Chin. J. Chem. Phys.* **2014**, *27*, 373–379.

(36) Jiang, B.; Guo, H. Relative efficacy of vibrational vs. translational excitation in promoting atom-diatom reactivity: Rigorous examination of Polanyi's rules and proposition of sudden vector projection (SVP) model. *J. Chem. Phys.* **2013**, *138*, 234104.

(37) Jiang, B.; Guo, H. Control of mode/bond selectivity and product energy disposal by the transition state: $X + H_2O$ ($X = H, F, O(^3P)$, and Cl) reactions. *J. Am. Chem. Soc.* **2013**, *135*, 15251–15256.

(38) Zhou, Y.; Zhang, D. H. Eight-dimensional quantum reaction rate calculations for the $H + CH_4$ and $H_2 + CH_3$ reactions on recent potential energy surfaces. *J. Chem. Phys.* **2014**, *141*, 194307.

(39) Davison, S.; Burton, M. Reaction of methyl radicals with hydrogen and deuterium. *J. Am. Chem. Soc.* **1952**, *74*, 2307–2312.

(40) Majury, T. G.; Steacie, E. W. R. The reactions of CH_3 and CD_3 radicals with hydrogen and deuterium. *Can. J. Chem.* **1952**, *30*, 800–814.

(41) Shapiro, J. S.; Weston, R. E. Kinetic isotope-effects in reaction of methyl radicals with molecular-hydrogen. *J. Phys. Chem.* **1972**, *76*, 1669–1679.

(42) Marshall, R. M.; Shahkar, G. Rate parameters for $CH_3 + H_2 \rightarrow CH_4 + H$ in the temperature-range 584–671 K. *J. Chem. Soc., Faraday Trans. 1* **1981**, *77*, 2271–2276.